Experimental study of the compressive-force path concept in prestressed concrete beams

Salek M. Seraj

Department of Civil Engineering, Bangladesh University of Engineering and Technology, Dhaka, Bangladesh

Michael D. Kotsovos

Department of Civil Engineering, National Technical University of Athens, Greece

Milija N. Pavlović

Department of Civil Engineering, Imperial College of Science, Technology & Medicine, SW7 2BU, UK

(Received February 1992; revised version accepted November 1992)

A physical model, based on the concept of the compressive-force path, is proposed for the realistic design of prestressed concrete members. The compressive-force trajectory, as defined by this model, is verified through experimental investigations. A test conducted on a prestressed concrete T-beam has revealed that designing such members to the current code provisions may lead to a brittle type of failure. On the other hand, a similar girder designed to the proposed model not only attained its full flexural failure load, but did so with an amount of transverse reinforcement significantly lower than that specified by current methods.

Keywords: prestressed concrete, compressive-force path, codes of practice, structural testing, finite element analysis

The compressive-force path (CFP) concept[1] has recently been put forward in an attempt to provide a rational and unifying basis for structural concrete design. It departs from established thinking in that, instead of relying on such concepts as the 'truss-analogy'[2,3], the 'aggregate interlock' mechanism[4,5] and the notion of the 'critical' section of a member, it gives consideration to the presence of multi-axial stresses in a concrete structure and recognizes the brittle nature of concrete at the material level. In the past, physical models have been proposed, in compliance with the concept of CFP for the realistic design of various statically determinate reinforced concrete (RC) members[6–8], as well as statically indeterminate skeletal structures.[9] It is the purpose of the present work to extend these models so as to encompass prestressed concrete (PSC) structural forms.

It is argued that a PSC beam at the ultimate limit state behaves like an RC beam, and since the physical model based on the CFP concept provides a realistic description of the features of an RC member[6], it follows that it can also be used, after slight modifications, to model PSC members. During the modification of the model, the effect of the large prestressing force that is present in a PSC member has been allowed for. The crack pattern at failure obtained from the experimentation of a PSC beam (PCB1 – furnished with only a nominal amount of transverse reinforcement and subsequently failing in shear) has been employed to confirm the CFP proposed by the model. This experimental finding has been complemented by finite element (FE) analysis. The load-carrying capacity, deformational response, fracture process and modes of failure of two additional PSC beams (one designed using the proposed (CFP) physical model (PCB2) and the other designed to the British code BS 8110[10] (PCB3)) have been examined in an attempt to associate the causes and the mechanisms involved in their failure.

Notation

a	shear span
A_s	area of longitudinal tension reinforcement which continues for a distance at least equal to d beyond section being considered
A_{sv}	area of transverse reinforcement
b_1	effective width (see *Figure A1*)
C	compressive force in concrete
d	effective depth (mm)
f_{cu}	uniaxial compressive cube strength of concrete
f_{cyl}	uniaxial cylinder strength

0141-0296/93/060439-13

f_u ultimate stress of tension steel (N mm^{-2})
f_y yield stress of tension steel (N mm^{-2})
f_{yv} yield stress of stirrup material
h horizontal projection of inclined portion of CFP
M_a applied bending moment (Nmm)
M_c moment corresponding to failure load (Nmm)
M_f flexural capacity (Nmm)
P_e effective prestressing force in tendons
P_i initial prestressing force in tendons
R reaction at support
s distance from support of cross-section at which M_c is calculated (mm) (equal to shear span for point loading, and $2d$ (in RC members) or h (in PSC members) for uniformly distributed loading)
T tensile force in longitudinal steel
T_{sv} transverse tensile force
V_a applied shear force
V_c tensile force resisted by concrete alone in region where CFP changes direction
X depth of neutral axis
x' depth of neutral axis considering triaxial conditions
X_g centroidal distance of uncracked concrete from compression face
z lever-arm distance
δ arbitrary length used in calculating A_{sv} per δ
Δz increase in lever arm
ϕ bar size
ρ_w tension steel ratio (A_s/bd)
σ'_c nominal triaxial compressive stress
σ_c $0.8 f_{cyl}$
σ_{conf} confining pressure required for σ_c to increase to σ'_c
σ_t transverse tensile stress

Design method

Physical model for PSC members

The concept of the CFP is based on a proper understanding of concrete as a material and, thus, provides a rational alternative for overcoming some of the deficiencies of current design thinking. On the basis of this concept, the load-carrying capacity of a structural concrete member is associated with the strength of concrete in the region of the paths along which compressive forces are transmitted to the support. The path of the compressive force may be visualized as a 'flow' of compressive stresses with varying section perpendicular to the path direction, the compressive force representing the resultant of the stresses at each section as shown in *Figure 1*. Failure has been shown to be related to the presence of tensile stresses in the region of the path and such stresses may develop due to a number of causes, the main ones being associated with changes in the path direction, the varying intensity of the compressive stress field along the path, bond failure at the level of the tension reinforcement between two consecutive flexural inclined cracks, etc.

In contrast to RC members, a large amount of additional compressive force in the form of prestressing is available in a PSC member; and, therefore, such a

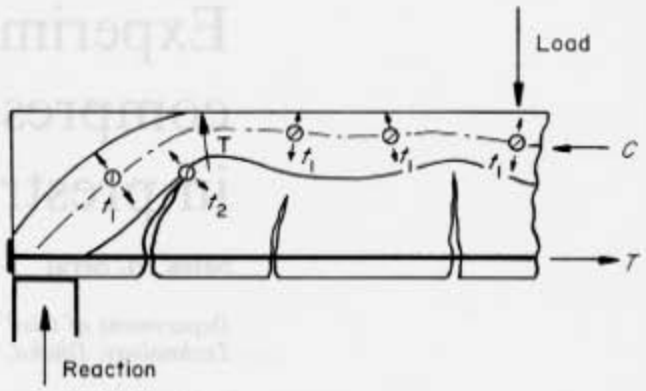

Figure 1 Schematic representation of compressive-force path

prestressing force should play a vital role in determining the nature of the CFP. In *Figure 2*, the 'frame-like' physical model developed for the design of RC beams[6] has been modified to cater for the effect of the prestressing force. The figure shows that the model comprises a frame with inclined legs, providing a simplified but realistic description of the shape of the CFP, and a number of 'teeth' representing concrete cantilevers, which form between consecutive flexural or inclined cracks within the beam web under increasing load. In this model, the length of the horizontal projection of the inclined leg of the compressive-force trajectory (h) has been considered to be primarily dependent on the ratio of the amount of effective prestressing force (P_e) and the vertical reaction (R) at the support level. It is suggested that, in a PSC beam, the inclined leg of the CFP at failure, takes the direction of the force resultant at the support. The length 'h' is, therefore, given by

$$h = (d - X_g) * P_e/R \tag{1}$$

where 'd' is the effective depth of the beam and 'X_g' is the distance of the centroid of the compression area from the top of the compression face. Unlike the case of RC beams[6], this simple relationship automatically takes care of the shear-span to depth (a/d) ratio, as the reaction 'R' is a function of the shear span 'a' (for a given flexural capacity) and 'd' is a constant; however, it should be noted that the value of R in equation (1) should correspond to the design (flexural or shear) mode of failure at the ultimate limit state. Otherwise, the value of R is clearly dependent on the type of loading. Although the model of *Figure 2* refers to PSC beams with a straight tendon profile, it can also be used for beams having inclined tendons, as employed later in this paper.

Failure criteria

To implement the preceding model in design, it is essential to complement it with a failure criterion. Such a failure criterion cannot be unique, since under the combined action of bending moment and shear force PSC beams may fail due to a number of causes before flexural capacity is attained, as mentioned earlier. An analytical description of these internal actions causing failure has already been derived empirically[11], and is shown, as slightly modified elsewhere[6], in Appendix 1.

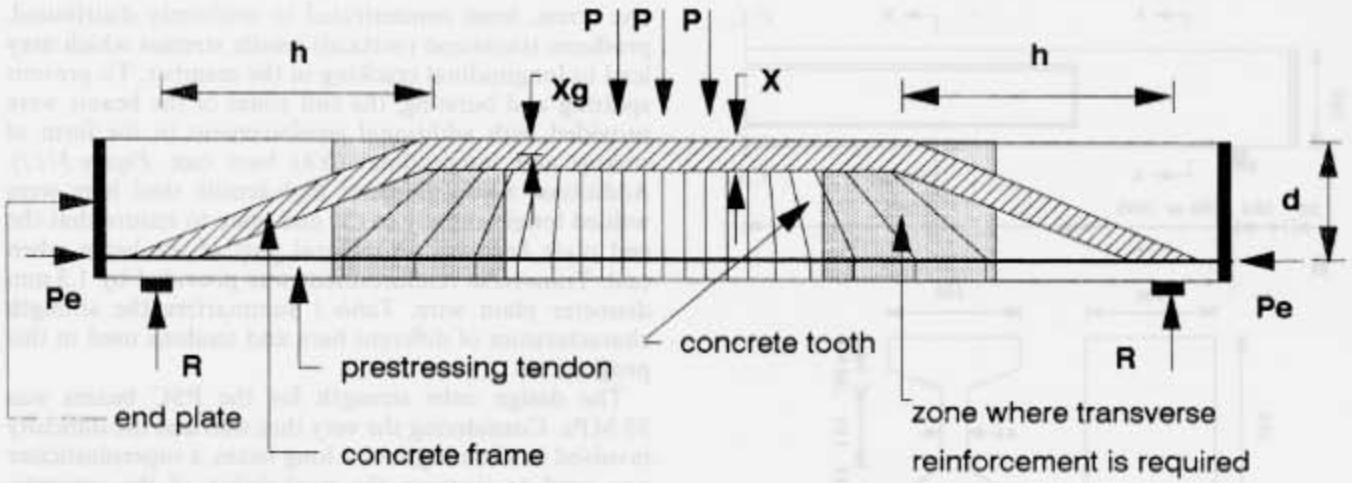

h = (d-Xg) * Pe / R

where,

h = horizontal projection of the inclined portion of the CFP

Pe = effective prestressing force

R = reaction at support

P = applied (point or uniformly distributed) load

d = effective depth of the member

Xg = centroidal distance of uncracked concrete from the compression face

Figure 2 Proposed frame model for prestressed concrete beam

Provision of transverse reinforcement

As indicated in Appendix 1, if the conditions for failure are fulfilled before flexural failure occurs, one of the design solutions that will allow the beam to attain its flexural capacity involves the provision of transverse reinforcement. It is important to note that shear reinforcement is only required in the region of the joint of the horizontal and inclined members of the frame, with a nominal amount being sufficient in the remaining portions of the PSC beam. The shear reinforcement is designed so as to sustain the portion of the tensile force, balancing the action of the compressive forces acting along the members, that cannot be sustained by concrete alone.

In PSC members, significant internal tensile actions may develop, for equilibrium purposes, within both the regions where the CFP changes direction and, for the case of point loading, the horizontal portion of the path in the region of point loads to sustain tensile stresses that may develop when bond failure occurs between two consecutive flexural or inclined cracks (bond failure will increase the depth of the right-hand crack, thus causing redistribution as indicated in *Figure A2* in Appendix 2). For simplicity, consider a rectangular cross-section. The resulting transverse tensile stresses, with the corresponding stress resultant and the amount of reinforcement required to sustain it, may easily be assessed as described in Appendix 2.

A full description of CFP models for RC and PSC members, together with design examples and experimental verification are available elsewhere[6,12]. For present illustration purposes, the relevant design details for beam PCB2 have been included in Appendix 3.

Experimental programme

The experimental work to be described here was intended not only to verify the proposed (CFP) physical model in the design of PSC members but also to identify probable inadequacies of the current shear design procedures. All the PSC T-beams reported in the present paper were initially prestressed to about 59% of the ultimate capacity of the prestressing tendons, with an estimated effective prestressing force of about 50% of the strength of the strands. It should be mentioned here that, in the original research programme[12], the proposed method was also verified by conducting both physical and numerical experiments on PSC members prestressed to an effective prestressing force of about 60% of the strength of the tendons; the relevant results are reported elsewhere[13,14].

Beam details

Broadly, two types of post-tensioned PSC beams were tested. The type I PSC beam (this consisted of a single test) was 6660 mm long, simply supported with a span of 6000 mm and subjected to two-point loading. The type II PSC beams were 5660 mm long, simply supported with a span of 5000 mm and subjected to six-point loading. Typical cross-sectional characteristics and end-zone reinforcement details of the PSC beams studied are given in

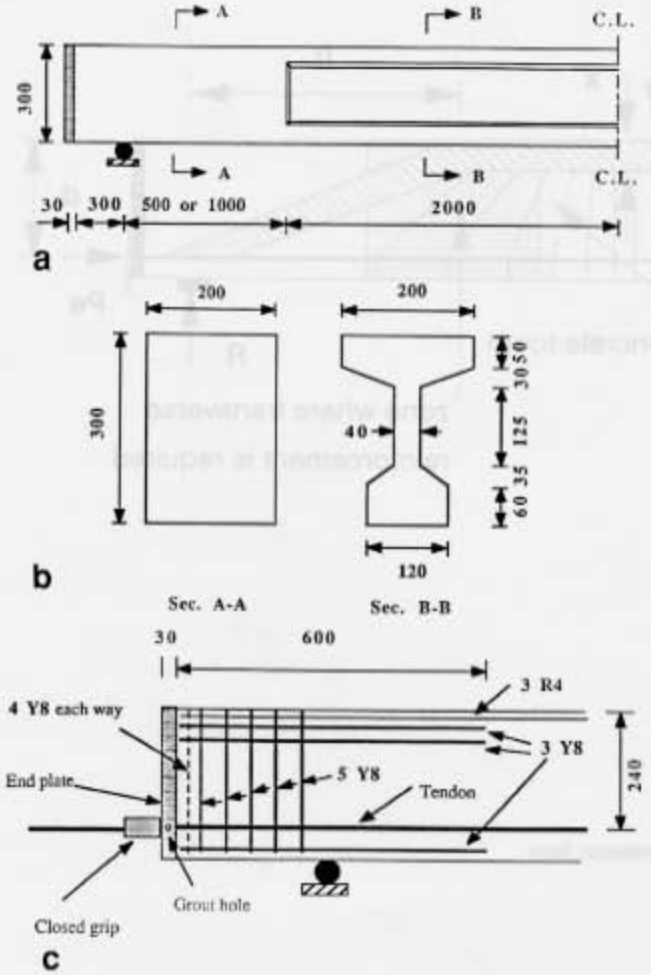

Figure 3 (a) and (b) cross-sectional characteristics; (c) reinforcement details of end zones of prestressed concrete beams tested in programme (all dimensions and bar sizes in mm)

Figure 3. All the type II PSC beams to be studied here possess a straight tendon profile, as shown in *Figure 3*. On the other hand, although the tendon profile for the type I PSC beam remains straight for most of its length, it does, in fact, make a small angle from a distance of 1030 mm from the end faces, ending at midheight of the end plate (see *Figure 4*). The depth of the tendons at the prestressing and support levels were 150 mm and 178.84 mm (as measured from the top of the beam), respectively. *Figure 4* also contains the CFP predicted on the basis of the proposed physical model. The slightly inclined tendon profile was adopted in an attempt to first test the applicability of the proposed model in a more complex (i.e. non-horizontal) tendon case, so that it could be applied to any arbitrary tendon profile later. The loading configurations to which the beams were subjected are shown in *Figure 5*.

The tensile reinforcement of the PSC beams comprised 12.9 mm diameter super steel strand wire conforming to BS 5896/3. Additional links and secondary reinforcement were provided in the flange of the beams. High-tensile steel of 6 mm diameter, mild steel of 4 mm diameter and 1.5 mm diameter were used for this purpose. The prestressing force in the post-tensioned beams under study was applied at the end face with the aid of mechanical anchorage. The transition of this longitudinal compressive stress, from concentrated to uniformly distributed, produces transverse (vertical) tensile stresses which may lead to longitudinal cracking in the member. To prevent splitting and bursting, the end zones of the beams were provided with additional reinforcement in the form of stirrup and longitudinal (Y8) bars (see *Figure 3(c)*). Additional 8 mm diameter high-tensile steel bars were welded longitudinally to the end plate to ensure that the end plate becomes an integral part of the beam when cast. Transverse reinforcement was provided by 1.5 mm diameter plain wire. *Table 1* summarizes the strength characteristics of different bars and tendons used in this programme.

The design cube strength for the PSC beams was 55 MPa. Considering the very thin web and the difficulty involved in vibrating such a long beam, a superplasticizer was used to increase the workability of the concrete. *Table 2* gives details of the mix proportions used.

A 22 mm diameter, properly aligned, galvanized iron duct was kept within the formwork before the casting of the beams. Two 200 mm wide, 300 mm high and 30 mm thick steel plates were used as end plates at each end of the beam. The plates were suitably drilled in accordance with the tendon profile, duct and end-anchorage size. On the sides of the plates, grout inlet/outlet holes were made. A grout having a water/cement ratio of 0.44, 1.01 of superplasticizer per 100 kg of cement, and a 100 gm pack of grout additive per bag of cement was used. The grout thus produced was found to be satisfactory from both workability and strength viewpoints.

The type I PSC beam PCB1 was tested in order to explore the nature of the compressive-force trajectory in a PSC member. It is clear that the cracking pattern of an under-reinforced PSC beam failing in shear can best portray the location of the change in trajectory of the CFP (for beams failing in flexure, this region remains largely uncracked). To test the basic ideas, the beam was neither designed to BS 8110, nor were the recommendations of the CFP concept implemented; such an approach ensured that the member would fail in shear and, thus, the web of the beam was furnished with nominal reinforcement only. This nominal reinforcement was

Table 1 Reinforcement characteristics

Type of reinforcement	f_y, MPa	f_u, MPa
12.9 mm ϕ stabilized strand	—	1980.4
8 mm ϕ high-yield steel	470	565
6 mm ϕ high-yield steel	570	665
4 mm ϕ mild steel	460	540
1.5 mm ϕ mild steel	460	510

Table 2 Concrete mix proportions (by weight) used in manufacture of PSC beams

Type	55 MPa mix
10 mm aggregate	3.15
Coarse sand	2.00
Fine sand	0.89
Cement	1.00
Water	0.58
Superplasticizer	1.20 litre/100 kg cement

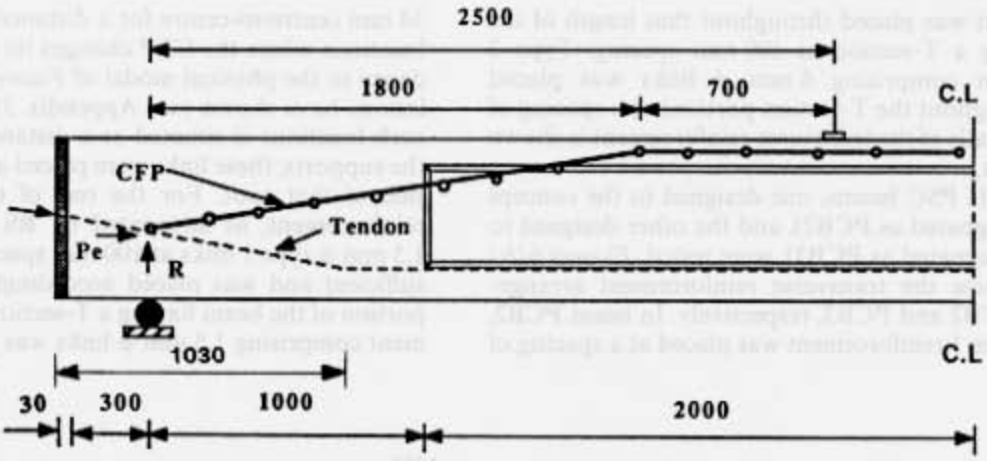

h = horizontal projection of the inclined leg of the model

= (d-Xg)Pe /R = (178.84-26.67) * 191183.3 / 16251.43

~ 1800 mm

Note: In this calculation, since the tendon was inclined, the horizontal component of the effective prestressing force has been taken as "Pe", the net upward force due to the action of prestressing and the reaction has been taken as "R", and the depth of the tendon at the support level has been taken as "d". All calculations refer to the ultimate limit state.

Figure 4 Inclined tendon profile and predicted CFP for PCB1 (all dimensions in mm)

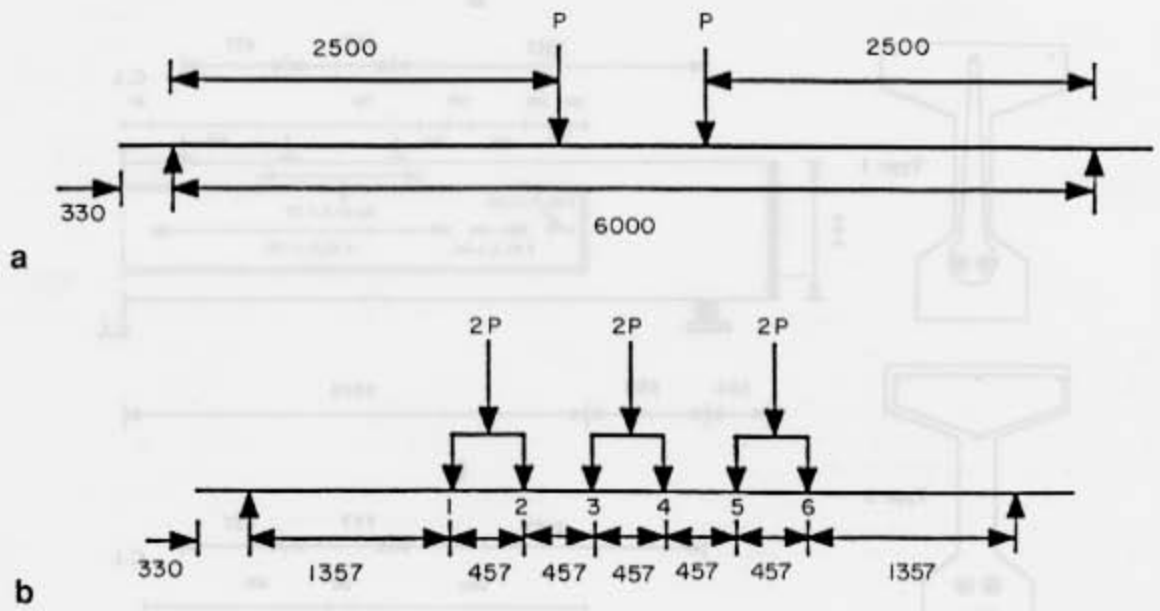

Figure 5 (a) Two-point and (b) six-point loading configurations (all dimensions in mm)

about 40% of the web reinforcement which is prescribed by BS 8110. On the other hand, this nominal web reinforcement could cater for only 60% of the transverse reinforcement (in accordance with the CFP design) needed at locations where the CFP changes its direction, in order to sustain the tensile force that may develop at these places. So far, both the BS 8110 and the CFP design requirements refer to flexural failure, whereas in this test a shear type of failure was sought. However, in order to guarantee that the planned shear failure takes place due to the (additional) tensile stresses at the location where the CFP changes direction, and not due to bond failure, the flange of the beam was furnished with an adequate amount of links, as can be calculated from CFP provisions.

The PSC beams tested had two types of transverse reinforcement. Type 1 consisted of two-legged links extending from the top face of the beam to the level of the prestressing tendon. Type 2 transverse reinforcement was a 'hoop-like' reinforcement placed around the top flange of the beams.

In type I PSC beam PCB1, 1.5 mm ϕ type 1 transverse

reinforcement was placed throughout that length of the beam having a T-section at 100 mm spacing. Type 2 reinforcement comprising 6 mm ϕ links was placed (again, throughout the T-section portion) at a spacing of 100 mm. Details of the transverse reinforcement is shown in *Figure 6(a)*.

Two type II PSC beams, one designed to the concept of CFP (designated as PCB2), and the other designed to BS 8110 (designated as PCB3), were tested. *Figures 6(b)* and *6(c)* show the transverse reinforcement arrangements for PCB2 and PCB3, respectively. In beam PCB2, 1.5 mm ϕ type 1 reinforcement was placed at a spacing of 34 mm centre-to-centre for a distance 'd' (= 240 mm) at locations where the CFP changes its direction, in accordance to the physical model of *Figure 2*. Since the calculations have shown (see Appendix 3) that the centre of such locations is situated at a distance of 920 mm from the supports, these links were placed at 120 mm on either side of that spot. For the rest of the beam, nominal reinforcement, as advocated by BS 8110, constituting 1.5 mm ϕ type 1 links at 100 mm spacing was considered sufficient and was placed accordingly throughout that portion of the beam having a T-section. Type 2 reinforcement comprising 1.5 mm ϕ links was placed at a spacing

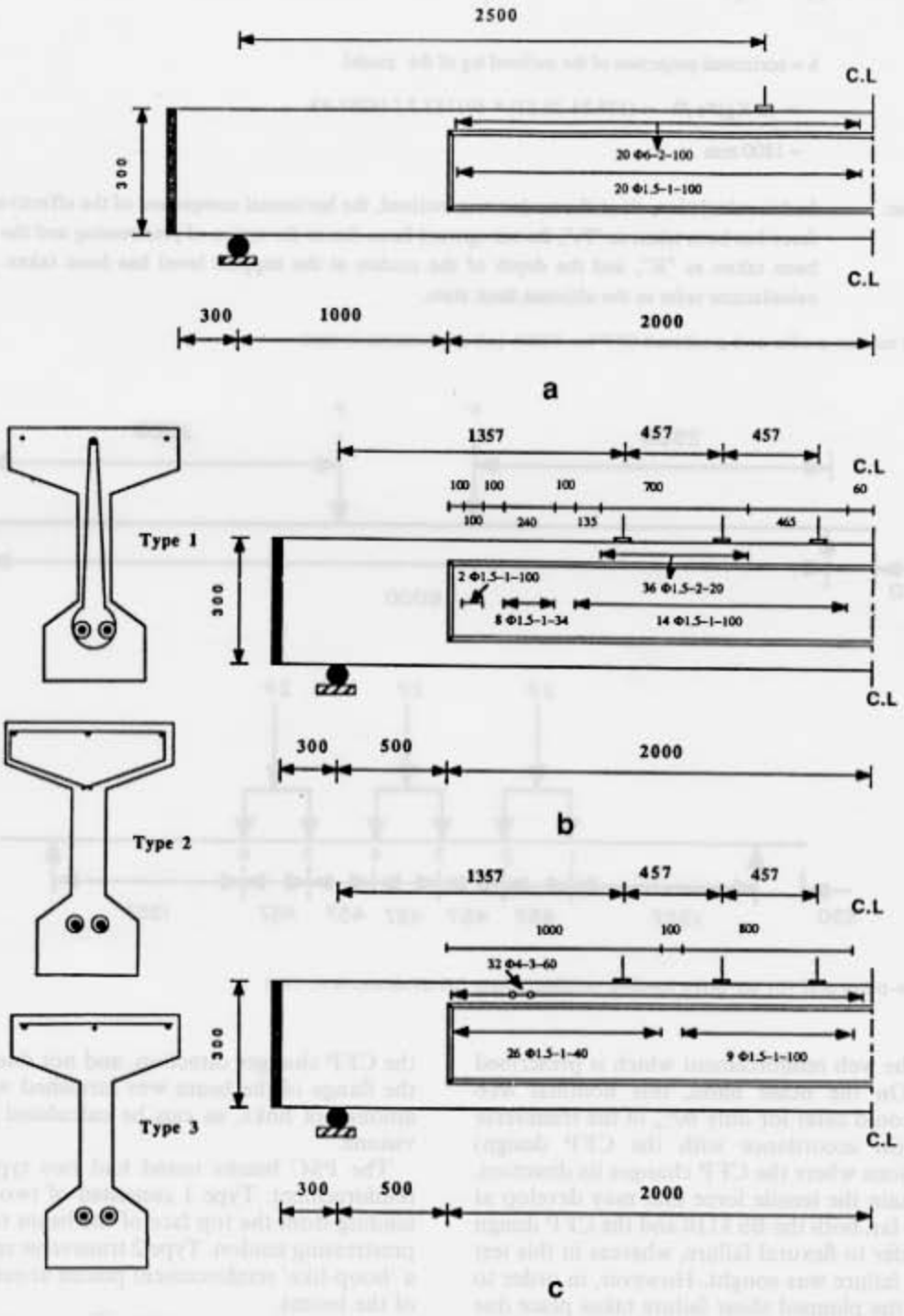

Figure 6 Transverse reinforcement details of (a) PCB1, (b) PCB2 and (c) PCB3 (all dimensions and bar sizes in mm)

of 20 mm from a distance of 120 mm before the first (and after the sixth) point-load to 120 mm after the second (and before the fifth) point-load.

In beam PCB3, 1.5 mm ϕ type 1 links were placed at a spacing of 40 mm centre-to-centre throughout the whole T-section length of the shear span subjected to maximum shear stress (this reinforcement was also extended about 140 mm beyond the first (and before the sixth) load point). For the rest of the beam, type 1 links were placed at a spacing of 100 mm. Apart from these, and as recommended by BS 8110, type 3 reinforcement consisting of a straight piece of 4 mm ϕ mild steel was placed at the top of the top flange, perpendicular to the longitudinal direction of the beam at a spacing of 60 mm.

The concrete strength characteristics of all these beams are given in *Table 3*. In the preliminary design calculation of the beams, 80% of the cube strength was assumed as the equivalent uniaxial cylinder compressive strength of the concrete. The actual cylinder strength was established on the day of testing. The detailed calculation regarding the assessment of web and flange reinforcement of all these beams is available elsewhere[12], while that of PCB2 may be found in Appendix 3.

Prestressing

The prestressing operation was carried out by means of a purpose-built rig (see *Figure 7* for prestressing end of the rig) consisting of two identical 20-ton jacks, CCL grips and other accessories. The jacks were energized together to stress both the tendons of the beams evenly. The prestressing process was monitored closely with the aid of several linear voltage differential transducers (LVDTs) and electrical resistance strain gauges. About one day after the completion of the prestressing exercise, the beams were re-prestressed and shims were inserted to cater for the losses due to slip at the jaws of the grips and due to initial relaxation. From the amount of final elongation of the tendons, the quantity of the initial prestressing force was found. The effective prestressing force was estimated after allowing for various prestressing losses. Further details concerning the prestressing operation can be found in Reference 12.

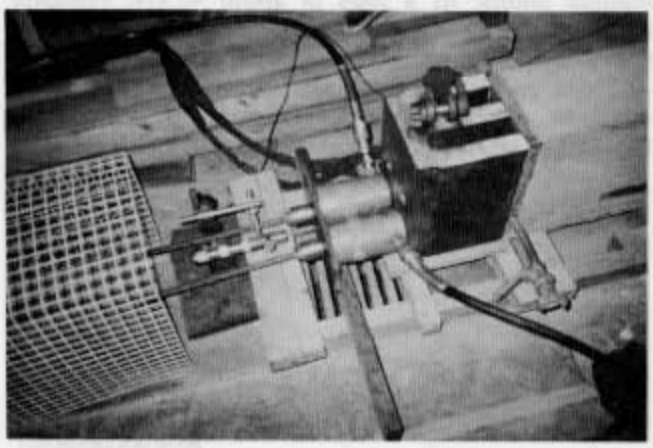

Figure 7 Outside view of prestressing rig

Testing

The two-point loading in the PSC beam PCB1 was applied through a hydraulic ram and a spreader beam supported on steel loading plates. In the case of other PSC beams subjected to six-point loading, three identical 20-ton jacks connected in series to an Amsler machine were commissioned. Beneath every hydraulic jack, one spreader beam supported on two steel loading plates was placed.

The midspan deflection, the 0.22 span deflection and the out-of-plane displacements were recorded. There were 2 LVDTs at the midspan, 2 on the sides to measure out-of-plane displacement and 1 LVDT at each of the 0.22 span locations from the support of the beam. At each load increment, the load was maintained constant for about 3 min in order to monitor the load and deformation response of the beam, mark the cracks (if any), and take photographs of the member's crack patterns. The measured values of load, displacement, and strain were recorded by a computer-logger capable of measuring to a sensitivity of $\pm$ 0.1 N, $\pm$ 0.0001 mm, and $\pm$ 12 micro-strains, respectively, with a speed of about 10 channels per second. Details of the prestressing, re-prestressing, grouting, loading, instrumentation, testing procedure, loading sequence, and the validation of the prestressing and testing set-ups are available elsewhere[12].

Discussion of results

Load-carrying capacity

The measured load-carrying capacity of all the PSC beams along with the CFP, BS 8110 and ACI 318-83[15] predictions are given in *Table 4*. From the table it can be seen that the type I beam PCB1 failed in shear at an applied load of 56 kN (57 kN including the load of the spreader beam). The British code predicted a shear failure at a load of 56 kN, while the proposed method predicted a failure load of about 61 kN. Thus, although both methods gave close predictions of the load-carrying capacity, the British code's value was the more accurate one.

Table 3 Concrete strength characteristics of various PSC beams tested

Beam	Age at test (days)	Cube strength (MPa)		Cylinder strength (MPa)
		28 days	Testing day	Testing day
PCB1 (Type I)	64	54.1	57.0	46.4
PCB2 (Type II)	72	55.3	57.4	46.2
PCB3 (Type II)	69	54.8	56.9	46.3

Table 4 Predicted and actual failure loads of PSC beams tested

Beam	Load type	Total sustained load, kN (failure type)			
		Predicted (kN)			
		BS 8110	ACI 318	CFP	Measured (kN)*
PCB1	Two-point	56.00 (brittle)	47.98 (brittle)	61.00 (brittle)	56.00 (brittle)
PCB2	Six-point	83.90 (brittle)	74.60 (brittle)	92.18 (ductile)	107.00 (ductile)
PCB3	Six-point	92.18 (ductile)	86.30 (brittle)	88.94 (brittle)	90.00 (quasiductile)

*add weight of spreader beam(s) (1 kN for PCB1 and 1.5 kN for PCB2 and PCB3) to obtain total sustained load

The type II beam PCB2 attained its flexural capacity at an imposed load of 107 kN. Although both the proposed method in compliance with the CFP concept and BS 8110 underestimated the flexural capacity in the course of the design calculations (15% by CFP and 23% by BS 8110), the amount of transverse reinforcement used was significantly smaller in the former case. For PCB2, the total amount of transverse reinforcement in the web was only 60% of that in PCB3 within the shear span subjected to the maximum shear force (i.e. in the T-section between the support and the loading points nearest to the supports, see points 1 and 6 in *Figure 5(b)*). However, in PCB2 additional links were provided in the flange in the region of loading points 1, 2 and 5, 6 (see *Figure 5(b)*) to cater for the tensile stresses that develop due to possible bond failure. Beam PCB3, on the other hand, had a uniform amount of shear reinforcement (in each shear span) as calculated by using BS 8110. PCB3 also had nominal reinforcement in the flange in the direction perpendicular to the longitudinal direction of the beam. Beams PCB2 and PCB3 both had the same cross-sectional dimensions, material properties and longitudinal reinforcement. Thus, the flexural capacity (based on triaxial properties) of both beams should have been essentially the same if shear (quasiductile) failure had not occurred in the BS 8110-designed member PCB3 at its calculated flexural capacity (based on uniaxial properties). The causes of the observed behaviour will be discussed later.

Deformational response

The load–deflection relationships obtained from the tests on PCB1, PCB2 and PCB3 are shown in *Figure 8*. Although two LVDTs (70 mm apart) recorded the midspan deflection of each of the beams, only readings of one of them have been shown in the figure, as they were almost identical[12], thus confirming that the loading was truly vertical and uniformly distributed across the width of the beam, with negligible torsional effects. The brittle nature of the failure of PCB1 can be seen from *Figure 8*. The ultimate failure loads for PCB2 predicted by the British code and the proposed method are also included in *Figure 8*. It can be seen that PCB2 exhibits a more ductile behaviour than PCB3, and that, in addition, PCB2 sustained about 19% more load than PCB3. Such a difference in the behaviour of these type II PSC beams can only be attributed to the effect of flange reinforcement and the provision of the necessary amount of web reinforcement at the relevant positions, since in all other respects both the PSC members were similar.

Cracking process

It is important to reiterate that the purpose of testing PCB1 was to visualize the ultimate crack pattern at failure, and to correlate such cracking pattern to the trajectory of the CFP. The cracking process was initiated by the formation of flexural cracks at the midspan of the beam at an applied load of about 30 kN. In the subsequent load step, the number of flexural cracks increased, and diagonal cracks were initiated in the web, near to the loading points. At a load of about 40 kN, extensive diagonal (shear) cracks were formed in the web of the beam. By the time the total applied load was about 45 kN, a pair of shear cracks, one in each shear span, which had reached the compression flange – web interface earlier, started moving along the said interface. At an

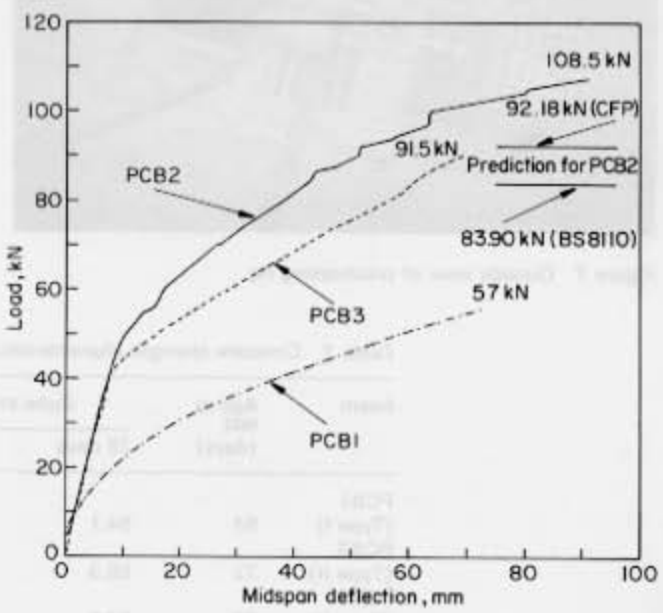

Figure 8 Load–deflection curves for PCB1, PCB2 and PCB3

applied load of 50 kN, these diagonal cracks started to open up. When the applied load reached 56 kN, the horizontal portion of one of the above-mentioned shear cracks penetrated into the flange of the beam, and eventually failure occurred. In *Figure 9*, the crack pattern after failure is shown; one should note that the crack width at failure was very large.

The cracking process for PCB2 and PCB3 has been described in detail elsewhere[12], by reference to photographs taken at significant stages of the crack-propagation sequence. Whereas the crack patterns just before failure for both the beams are given in *Figure 10*, the final crack patterns in the regions where the failure ultimately took place in these members appear in *Figure 11*. The summary of the cracking process is as follows. The first flexural crack in PCB2 took place at the midspan of the beam at 50 kN, i.e. at about 47% of the ultimate failure load. This crack propagated vertically upwards from the bottom face of the beam. As the load increased, a few similar cracks appeared adjacent to this first crack, the number of cracks increasing with increase in load. Some of the previously seen vertical cracks penetrated into the web and, also, new inclined cracks developed in the web. The rate of crack propagation and formation of new cracks drastically reduced at about 85 kN, i.e. at about 79% of the ultimately sustained load. At this stage almost all the web cracks propagated to the underside of the flange but did not penetrate into it. Although the cracking process stabilized at this stage, the rate of increase in the deflection of the beam did not reduce. At about 105 kN, flexural failure was almost imminent. When the load reached 107 kN, the flexural crack that had initially formed first, and which previously had reached the compression flange–web interface, suddenly became slightly inclined, and eventually failure occurred as the crack penetrated deep into the middle zone of the compression flange of the beam.

In the case of PCB3, the cracking process was initiated at 45 kN i.e. at about 50% of the failure load, when the first flexural crack was perceived. As the load increased, a few additional vertical cracks appeared nearby. At 55 kN, one pair of shear cracks, formed at symmetrically opposite positions in the web, moved very near to the underside of the flange. In the next few load increments of 5 kN each, more and more shear cracks appeared and

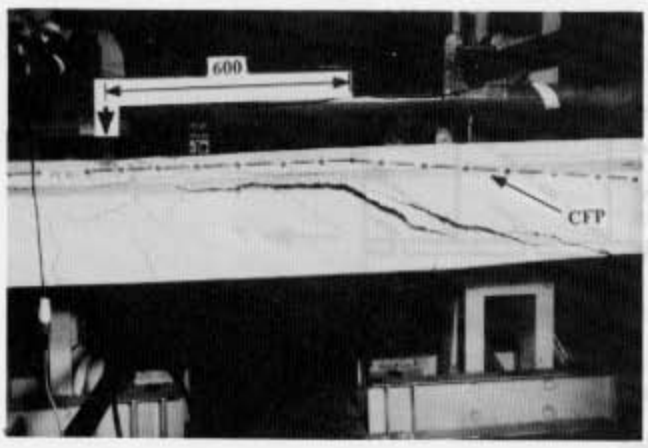

Figure 9 Crack pattern at failure and observed CFP of PCB1 (dimension is in mm)

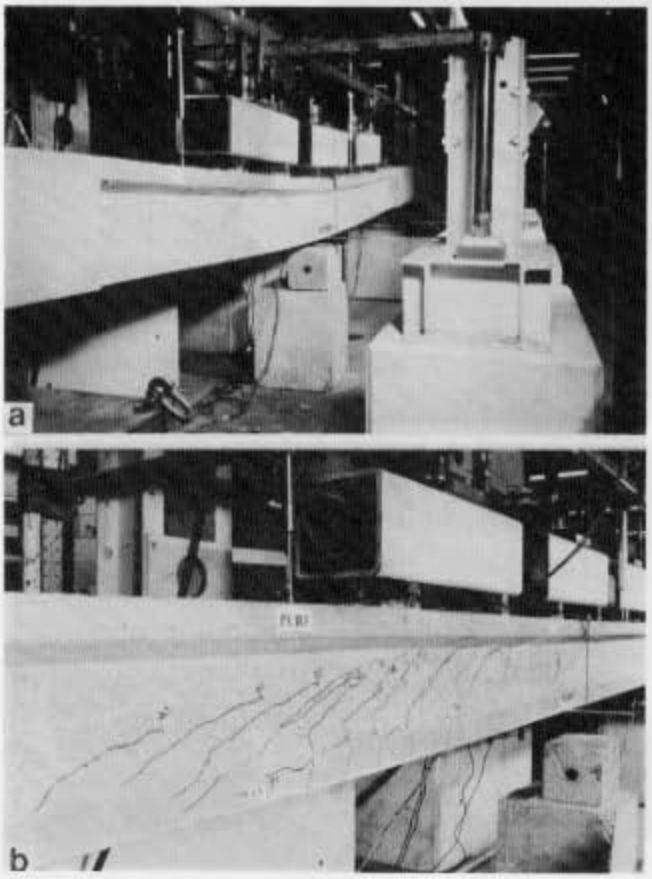

Figure 10 Crack patterns just before failure for (a) PCB2 (105 kN) and (b) PCB3 (90 kN)

flexural cracks went deep into the underside of the flange. By the time the beam sustained an applied load of 75 kN, some of the shear cracks near the second and the fifth loading points (see *Figure 5(b)*) started penetrating into the compression flange. At a load of 90 kN (84% of the true (or triaxial) flexural capacity exhibited by the similar type II PSC beam PCB2), there were shear cracks along the whole length of the beam and some of the large shear cracks penetrated deep into the flange (*Figure 10(b)*). The beam could not sustain any load beyond this level and eventually shear failure took place without prior warning.

Causes of observed behaviour and failure mechanism

The shear failure of PCB1, designed to fail in shear, is understandable. While the failure load was quite accurately predicted by the BS 8110 formula, the proposed method slightly over-predicted it. However, even though, in the present case, the British code has predicted the failure load well, the concepts that form the basis of such predictions remain questionable. According to the code, the design ultimate shear resistance of concrete was 24.15 kN[12]. This shear resistance provided by concrete, supposedly includes the contribution of aggregate interlock, which the present codes of practice consider to be substantial. The excessive width of shear cracks (virtually see-through cracks) near failure, however, clearly raises doubts on any possible presence of aggregate interlock at this stage. The share of the concrete contribution to shear resistance offered, according to current codes, by the

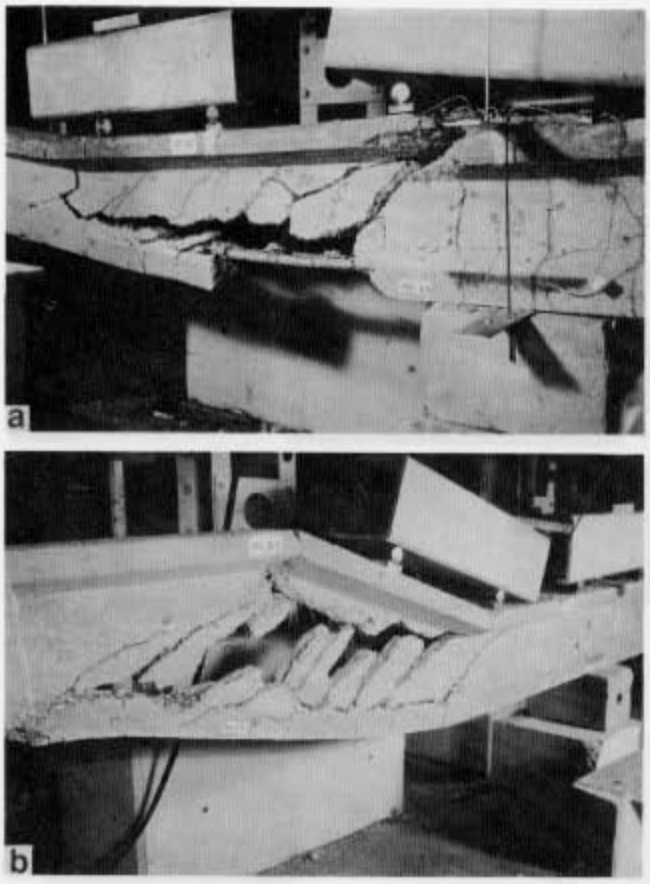

Figure 11 Crack patterns in regions where failure occurred for (a) PCB2 (failure at 107 kN); (b) PCB3 (failure at 90 kN)

aggregate-interlock mechanism, therefore, must have been borne by the concrete in the compressive zone since the so-called tension tie (stirrups) of the truss (see *Figure 12* for the truss model widely postulated by current design thinking) was at yield even before the attainment of maximum load and hence this transverse reinforcement could not have provided any additional shear-carrying capacity.

On the other hand, the final crack pattern of *Figure 9* shows that the diagonal crack, which ultimately led to the collapse of PCB1, started at about 1300 mm from the support, and after developing the inclined portion in the web, propagated horizontally along the web–flange interface. The intersection of the horizonal and the inclined portion met, approximately, at a distance of about 600 mm from the load point, i.e. 1900 m from the support. The trajectory of the compressive force was found by joining the location of the tendon at the support with this intersection of the horizontal and the inclined cracks and then extending it horizontally along the compression-flange; the resulting observed CFP has been indicated in *Figure 9* by a dot-dash line. In *Figure 4*, the CFP, as predicted by the proposed method, has already been shown. The resemblance between the proposed and the observed CFP is remarkable. There is, however, a gap of about 100 mm between the predicted and the observed location at which the CFP changed its direction. In the calculation shown in *Figure 4*, the reaction at the support has been estimated at the ultimate limit state, considering flexural failure, of the beam. Since the beam failed in shear at a load lower than its flexural failure load, the change point of the CFP moved slightly away from the predicted location. Error in judging the prestressing losses may also affect such calculations. It is worth mentioning here that a numerical simulation of the test results of PCB1 has also confirmed the proposed nature of the CFP in a PSC member[12,14]. In this simulation exercise, a recently developed fully three-dimensional finite-element (FE) package[16], the wide ranging applicability of which has been proven on the basis of several case studies of varying complexities[17,18] and concrete strengths[19], was employed. Since detailed description of the FE modelling (i.e. FE discretization, analytical crack patterns, load–deformational behaviour) of PCB1 are available elsewhere[12,14], they are not included here. *Figure 13* shows the analytical crack pattern at failure (at the maximum sustained load level) of PCB1. If the symbols comprising either crosses or circle with oriented dash (i.e doubly-cracked zones) are connected by a hypothetical line (shown dotted in *Figure 13*), the cracking pattern at failure can be visualized; and, in turn, from it the location of the change in CFP trajectory may be estimated. This location where the CFP changes direction is marked by the Gauss point having a circle with a diagonal crack. It can also be seen that numerical prediction of the crack pattern matches quite closely the experimental failure pattern of *Figure 9*. It is, therefore, apparent that the failure of PCB1 was due to the pro-

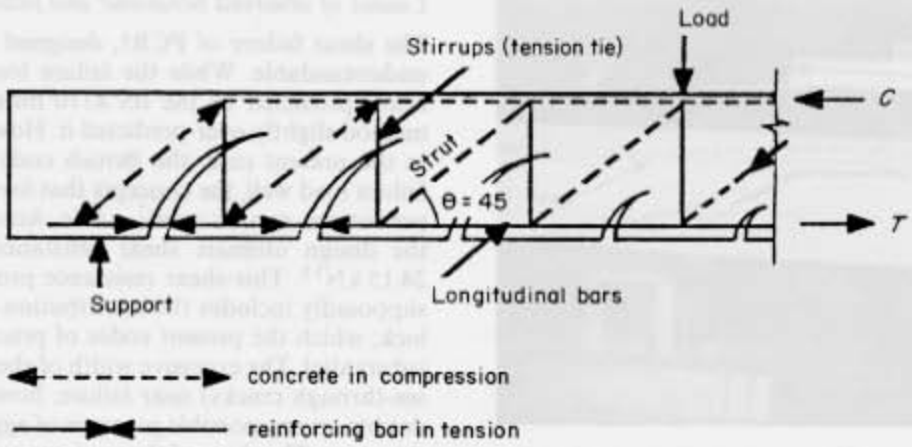

Figure 12 Truss model

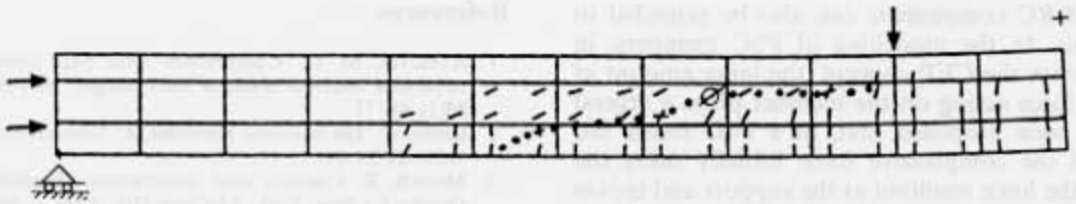

Figure 13 Beam PCB1. Analytical crack pattern at maximum sustained load level. (Dotted trajectory joins doubly-cracked zones and indicates ultimate failure pattern. Location where CFP changes direction is marked by Gauss point having a circle with a diagonal crack; CFP trajectory can be visualized by first drawing a straight line between support at tendon level (3/5ths of beam height from top face) and Gauss point in question, and then another line extending from this point above dotted line and roughly parallel to it.)

vision of an inadequate amount of transverse reinforcement at places where the CFP changed its direction.

As mentioned earlier, current design methods are usually based on the truss-analogy concept. According to this school of thought, a reinforced or prestressed concrete beam behaves as a truss once inclined cracking occurs, with the transverse reinforcement forming the ties while concrete between the consecutive inclined cracks acts as a strut. On the basis of the above concept, beam PCB3 should transform into a truss, after shear cracks are formed, which should be stronger than the truss that would be formed out of PCB2. Thus, PCB3 should sustain more load than PCB2. However, in reality the reverse happened. Beam PCB2 sustained 19% more load than PCB3 and attained its flexural capacity while beam PCB3 failed in 'shear' (in a quasiductile manner). Such a behaviour indicates that truss behaviour is not a necessary condition for a PSC member to attain its flexural capacity, once the shear capacity of the concrete is exceeded. It is interesting to note that beam PCB3 could not attain its true (triaxial) flexural capacity (as had been the case with PCB2) even though it just sustained the load corresponding to the calculated flexural capacity (based on uniaxial properties). This clearly shows that the present code provisions, which try to advocate the truss-analogy concept to model a beam under shear force, without giving proper attention to the stress conditions in the path through which the compressive force is transmitted from the load point to the support, may result in this type of undesirable failure. It is also apparent that, in a PSC beam, provision of reinforcement according to the CFP concept gives results that are much better than the presently available code provisions. The proposed method took care not only of the tensile forces developing where the CFP changes its direction but also of the (additional) tensile forces that can be developed in the flange due to bond failure at locations where both shear and moment are more prominent.

A closer look at the cracking process[12] provides a rational explanation of the observed failure mechanism. It appears that the absence of transverse reinforcement, in the flange of PCB3, prevented the beam from achieving a ductile deformational response, as shear cracks penetrated into its compression flange at loads as early as 75 kN. A comparison between the cracking patterns just before failure of PCB2 and PCB3 shows in the latter the presence of horizontal cracks (*Figure 10(b)*) at the interface of the web and bottom-flange (i.e. at the height of tendons) suggesting bond failure, while no such cracks are exhibited in the former (*Figure 10(a)*). Bond failure results in an increase in the length of the lever arm (see *Figure A2* in Appendix 2), which in turn necessitates an enhancement in the average compressive strength of the concrete. Since the compression flange of PCB3 was not furnished with transverse reinforcement in the form of hoops, it was not capable of providing adequate confinement required for such improvement in the concrete strength. As a result, cracks could penetrate into the flange without any difficulty. Now, while inadequate flange confinement initiates much of the critical cracking (*Figure 10(b)*), it is the crack at the location where the CFP changes direction (*Figure 11(b)*) which produces failure. Due to the absence of the required amount of transverse reinforcement at the changing points of the CFP, the tension that develops at such locations could not be sustained by the beam PCB3. As a result, failure took place. *Figure 11(b)* clearly shows the snapping of the web reinforcement and the opening up of the web, at failure, in the locality where the CFP changes its direction. On the other hand, the absence of any such snapping of the transverse reinforcement in the critical shear span of the beam PCB2 (shown in *Figure 11(a)*), at failure, demonstrates the fact that the beam could sustain the above-mentioned tensile stresses, as an adequate amount of reinforcement was available at the critical positions. The beam, consequently, failed in a ductile fashion. It is obvious that the transverse reinforcement, in the flange of PCB2, also played an important role by confining the concrete there, and thus preventing the cracks from penetrating into the flange at the early stages of the failure process.

The calculation of the 'full' or 'true' flexural capacity of beam PCB2 from the ultimately sustained load also reveals that the neutral axis near failure was very close to the top face of the flange. This phenomenon can only be explained if the stress condition in the flange was one of triaxial compression and not, as widely believed, uniaxial compression. It should be noted that, due to triaxial compression, concrete in the compressive region fails at a much higher load than its uniaxial compressive strength, thus allowing the lever arm to increase its length. Consequently, the true or triaxial flexural capacity becomes higher than its uniaxial counterpart.

Conclusions

The following tentative conclusions can be drawn from the, admittedly, limited number of tests reported in this paper. It is to be noted, however, that the present findings have been confirmed by additional test results published elsewhere[13].

The physical model proposed by the CFP concept for

the design of RC components can also be extended to PSC elements. In the modelling of PSC members, in compliance with the CFP concept, the large amount of prestressing force acting on the member plays a crucial role. It has been proposed that, in a PSC beam, the trajectory of the compressive force initially takes the direction of the force resultant at the support and moves horizontally after reaching the centroid of the uncracked compression area. This CFP predicted by the proposed method has been found to be compatible with the experimentally and analytically observed crack pattern.

The attainment of the full potential flexural capacity by the PSC beam designed in compliance with the CFP concept using the proposed physical model appears to be a promising way forward for achieving a rational design. It also indicates that the proposed (CFP) method of designing concrete structures is equally applicable to both RC and PSC members, thus providing a unifying feature in structural-concrete design thinking.

On the other hand, the beam designed to BS 8110 failed to achieve a true (triaxial) flexural failure and underwent a quasiductile deformational behaviour even though it contained about 40% more web reinforcement than the beam designed to the CFP concept (which, however, had additional flange reinforcement). The British code predicted the failure load of this beam quite accurately (although this was about 19% less than the failure load of the beam designed to the CFP concept, which apparently attained its true flexural capacity). The performance of this PSC beam designed to BS 8110 questions, once again, the validity of the truss-analogy concept, which ignores the presence of multiaxial stresses in structural concrete members. The final crack pattern of the latter beam justified the necessity of providing adequate transverse steel to cater for the tensile stresses that develop at locations where the CFP changes its direction.

Current design methods appear to be unsafe, since compliance to such codes may lead to a brittle type of failure. It appears that 'truss' behaviour is neither a necessary nor a sufficient condition for a PSC member to attain ductile failure. Instead, the consideration of the stress state in the compressive force trajectory seems to lead to a safer design solution.

Considering the fact that the amount of prestressing losses is not a fixed quantity, it might be good practice to spread the design transverse reinforcement over a wider length (say, for a distance '$2d$' instead of the presently applied length 'd') at locations where the proposed model predicts the CFP change in direction. This approach has been adopted in a further series of PSC beam tests, reported elsewhere[13].

Acknowledgments

The authors wish to thank the Science and Engineering Research Council, UK for financing the experimental work reported in this paper. The first author would like to express his gratitude to the Association of Commonwealth Universities, UK, for awarding him a Commonwealth Scholarship to carry out research of which the present work forms part. Thanks are also due to Bangladesh University of Engineering and Technology for granting him leave of absence during this research programme.

References

1 Kotsovos, M. D. 'Compressive force path concept: basis for reinforced concrete ultimate limit design,' *ACI Struct. J.* 1988, **85**(1), 68–75
2 Ritter, W. 'Die Bauweise Hennebique', *Schweizerische Bauzeitung*, 1899, **33**, 59–61
3 Mörsch, E. *Concrete steel construction*, (English transl. E. P. Goodrich,) New York, McGraw-Hill, 1909, p 368 (Translation from 3rd edn of *Der Eisenbetonbau*, 1st edn 1902)
4 Fenwick, R. C. and Paulay, T. 'Mechanism of shear resistance of concrete beams,' *J. Struct. Div, ASCE*, 1968, **94**(10), 2325–2350
5 Regan, P. E. 'Shear in reinforced concrete beams', *Mag of Concrete Res.* 1969, **21**(66), 31–42
6 Kotsovos, M. D. and Lefas, I. D. 'Behaviour of reinforced concrete beams designed in compliance with the concept of compressive force path,' *ACI Struct. J.* 1990, **87**(2), 127–139
7 Lefas, I. D., Kotsovos, M. D. and Ambraseys, N. N. 'Behaviour of reinforced concrete structural wall: strength, deformation characteristics and failure mechanisms', *ACI Struct. J.* 1990, **87**(1), 23–31.
8 Seraj, S. M., Kotsovos, M. D. and Pavlović, M. N. 'Behaviour of high-strength mix reinforced concrete beams (in preparation)
9 Seraj, S. M., Kotsovos, M. D. and Pavlović, M. N. 'Application of the compressive-force path concept in the design of reinforced concrete indeterminate structures: a pilot study,' (in preparation)
10 BS 8110 Structural use of concrete: Part 1: Code of practice for design and construction, British Standards Institution, London, 1985
11 Bobrowski, J. and Bardhan-Roy, B. K. 'Method of calculating the ultimate strength of reinforced and prestressed concrete beams in flexure and shear,' *Struct. Eng*, 1969, **47**, 197–209
12 Seraj, S. M. 'Reinforced and prestressed concrete members designed in accordance to the compressive-force path concept and fundamental material properties, PhD Thesis, Imperial College, London, 1991
13 Seraj, S. M., Kotsovos, M. D., and Pavlović, M. N. 'Compressive-force path and behaviour of prestressed concrete beams, *Mat. & Struct, RILEM*, 1993, **26**, 74–89
14 Seraj, S. M., Kotsovos, M. D., and Pavlović, M. N; 'Nonlinear finite-element analysis of prestressed concrete members,' *Proc. ICE, Structures and Buildings*, 1992, **94**, 403–418
15 Building code requirements for reinforced concrete, ACI 318-83, American Concrete Institute, Detroit, 1983
16 González Vidosa, F., Kotsovos, M. D. and Pavlović, M. N. 'A three-dimensional nonlinear finite-element model for structural concrete, part 1: main features and objectivity study,' *Proc. ICE (Part 2)* 1991, **91**, 517–544
17 González Vidosa, F., Kotsovos, M. D. and Pavlović, M. N. 'A three-dimensional nonlinear finite-element model for structural concrete, part 2: generality study' *Proc. ICE (Part 2)* 1991, **91**, 545–560
18 González Vidosa, F., Kotsovos, M. D. and Pavlović, M. N. 'Nonlinear finite-element analysis of concrete structures: performance of a fully three-dimensional brittle model,' *Comput. & Struct.* 1991, **40**(5), 1287–1305
19 Seraj, S. M., Kotsovos, M. D. and Pavlović, M. N. 'Three-dimensional finite-element modelling of normal-and high-strength reinforced concrete members, with special reference to T-beams, *Comput. & Struct.*, 1992, **44**(4), 699–716

Appendix 1

Failure criterion

$$M_c = 0.875\, sd \left(0.342\, b_1 + 0.3 \frac{M_f}{d^2} \sqrt{\left(\frac{z}{s}\right)} \left(\frac{16.66}{\rho_w f_y}\right)^{1/4} \right) \qquad \text{(A1.1)}$$

where the various parameters are defined in the Notation and in *Figure A1*.

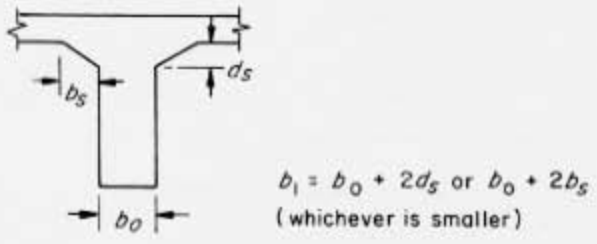

Figure A1 Definition of b_1 used in equation (A1.1)

Equation (A1.1) may be used in PSC member design as follows:

(1) Select cross-section s
(2) Find moment M_a at cross-section s due to applied loading
(3) Design cross-section s to sustain a given M_f
(4) Determine M_c from equation (A1.1); if $M_c > M_a$ only nominal stirrups would be needed
Otherwise, if $M_c < M_a$, either increase area of prestressing steel (thus increasing M_c to a level greater than or equal to M_a), or increase the cross-section; the alternative is to provide transverse reinforcement in accordance with the requirements described in Appendix 2

Appendix 2

Assessment of transverse reinforcement

(a) *Region where CFP changes direction*
Excess tensile force $T_{sv} = V = V_a - V_c$

$$V_c = M_c/s \qquad \text{(A2.1)}$$

Transverse reinforcement over a length d to sustain T_{sv} will be, $A_{sv} = T_{sv}/f_{yv}$
where the various parameters are defined in the Notation.

(b) *Horizontal portion of path (see Figure A2)*
Using information in *Figure A2*, the following steps are used:

(1) $\Delta z = V * X/(2T)$; $V = V_a - V_c$
(2) $x' = 2(d - z - \Delta z) > 0$; if $x' < 0$, increase cross-section

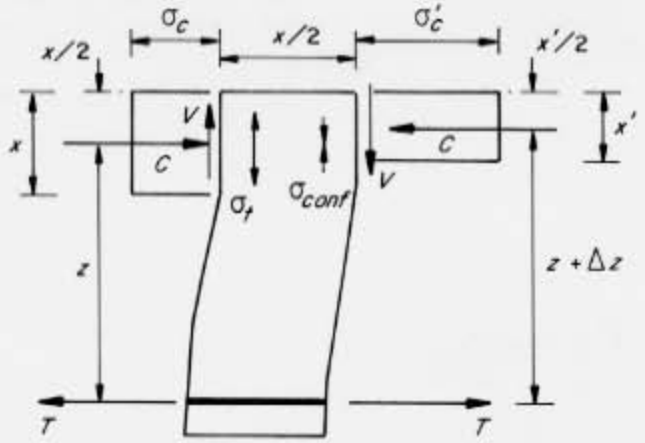

Figure A2 Assessment of excess tension due to bond failure

(3) Assess nominal triaxial compressive stress σ'_c
$\sigma'_c = C/(bx')$
(4) Assuming $0.8 f_{cyl}$ describes uniaxial condition ($\sigma_c = 0.8 f_{cyl}$), assess confining pressure σ_{conf} required for σ_c to increase to σ'_c, from expression $\sigma_{conf} = (\sigma'_c - 0.8 f_{cyl})/5$
(5) Assume transverse tensile stress $\sigma_t = -\sigma_{conf}$ (compression positive)
(6) Tensile force over length δ will be $T_{sv} = \sigma_t * b * \delta$
(7) Amount of transverse reinforcement over length δ to sustain tension T_{sv} will be $A_{sv} = T_{sv}/f_{yv}$

Appendix 3

CFP method design calculations for PCB2

Flexural capacity (see Figure 3)
$A_s = 205.4$ mm^2; $f_u = 1908.4$ N mm^{-2} gives, $T = 391985.3$ N
$f_{cu} = 55$ N mm^{-2} gives $\sigma_c = 0.67 f_{cu} = 36.85$ N mm^{-2}
Since $C = T$, $A_c = 391985.3/36.85 = 10637.32$ mm^2
Thus $X = 53.5$ mm and $X_g = 26.67$ mm
Lever arm, $z = 240 - 26.67 = 213.33$ mm
Hence flexural capacity $M_f = 391985.3 * 213.33 = 83621580$ N mm
Maximum total sustained six-point load as indicated in *Figure 5(b)* is $6 * 15361.73$ N
Shear force sustained by concrete
Shear span $s = 1357.5$ mm
Using equations (A1.1) and (A2.1), $M_c = 47128960$ N mm and $V_c = 34717.47$ N
Applied bending moment at $s = 1357.5$ mm, $M_a = 62561140$ N mm $> M_c$
Thus shear reinforcement is required. The location around which the compressive-force path will change its direction can be determined with the aid of the proposed model of *Figure 2*
Initial prestressing force, $P_i = 0.59 * T = 231271.3$ N
Considering 14% losses, effective prestressing force, $P_e = 0.86 * P_i = 198893.4$ N
Thus, using equation (1), $h = (d - X_g)P_e/R = (240 - 26.67) * 198893.4/46085 = 920$ mm
Transverse reinforcement

(i) For excess tension due to change in path direction [see Appendix 2(a)]
$T_{sv} = 46085.19 - 34717.47$ N $= 11367.72$ N
$A_{sv} = 11367.72/460 = 24.71$ mm^2
Provide $8\phi 1.5 - 1 - 34$, as shown in *Figure 6(b)*

(ii) For excess tension due to bond failure [see Appendix 2(b)]
$\Delta z = (46085.19 - 34717.47) * 53.5/(2 * 391985.3) \sim 1$ mm
$x' = 2(240 - 213.33 - 1) = 51.34$ mm
$\sigma'_c = 391985.3/(200 \times 50) = 39.2$ Nmm^{-2}, omitting tapered part
$\sigma_{conf} = 0.47$ N mm$^{-2} = -\sigma_t$
Tensile stress resultant over a length of 100 mm $= 0.47 \times 200 \times 100 = 9400$ N
Required reinforcement is $A_{sv} = 9400/460 = 20.43$ mm^2
Use $\phi 1.5 - 2 - 20$, as shown in *Figure 6(b)*